

Provided for non-commercial research and educational use only.  
Not for reproduction or distribution or commercial use.



This article was originally published in a journal published by Elsevier, and the attached copy is provided by Elsevier for the author's benefit and for the benefit of the author's institution, for non-commercial research and educational use including without limitation use in instruction at your institution, sending it to specific colleagues that you know, and providing a copy to your institution's administrator.

All other uses, reproduction and distribution, including without limitation commercial reprints, selling or licensing copies or access, or posting on open internet sites, your personal or institution's website or repository, are prohibited. For exceptions, permission may be sought for such use through Elsevier's permissions site at:

<http://www.elsevier.com/locate/permissionusematerial>

Short communication

## The study on transient characteristic of proton exchange membrane fuel cell stack during dynamic loading

Xiqiang Yan, Ming Hou\*, Liyan Sun, Haibo Cheng, Youlu Hong, Dong Liang, Qiang Shen, Pingwen Ming, Baolian Yi

*Dalian Institute of Chemical Physics, Chinese Academy of Sciences, Dalian 116023, China*

Received 22 August 2006; received in revised form 21 September 2006; accepted 21 September 2006

Available online 13 November 2006

### Abstract

The operations of fuel cell stacks in fuel cell vehicle are dynamic. During dynamic loading, the oxidant starvation often occurs, due to the gas response rate lagging the loading rate. To study the transient behavior of the fuel cell stack at load changes, the measuring methods of current and temperature distribution are developed. In this paper, the current distribution and temperature distribution as well as their dynamic changes in fuel cell stack have been evaluated in situ. The experimental results show that the local current and temperature rise when load rapidly. The extent of temperature fluctuation during dynamic loading is significantly influenced by air stoichiometries, loading rates, and air relative humidities. When air stoichiometry is very low, the temperature of cathode inlet rises sharply. The quicker the loading rate is, the bigger the extent of temperature fluctuation is. With increasing air relative humidity, the transient temperature of cathode inlet rises, while the transient temperature of cathode outlet decreases. This paper will provide reference for durability researches on fuel cell vehicles (FCVs).

© 2006 Elsevier B.V. All rights reserved.

**Keywords:** PEMFC; Dynamic loading; Current distribution; Temperature distribution

### 1. Introduction

The depletion of fossil fuels and the degradation of the environment have led to an interest in hydrogen as a fuel for transportation applications. The proton exchange membrane fuel cell (PEMFC) possesses several highly advantageous features such as a low-operating temperature, sustained operation at high current, low weight, potential for low cost and volume, fast start up, and suitability for discontinuous operation [1–4]. These features currently make the PEMFC as the most promising and attractive candidate for electric vehicle power [5–7]. Successful commercialization and acceptance of fuel cell power systems will demand that these products are as durable and reliable as existing internal combustion engine. [8].

Because operations of fuel cell stacks in fuel cell vehicles (FCVs) are dynamic, the transient behavior at load changes should be considered for the control, design, and optimum operation of fuel cell stacks. These transient operations may result

in the oxidant starvation due to gas response rate lagging the loading rate, which will affect the durability and reliability of fuel cell stacks further [9–12]. So improving on dynamic characteristics of fuel cell has become the key for prolonging FC life in FCV application. However, most of the studies of PEMFCs focused on steady operation, only a few authors considered transient behaviors of stacks [13–17]. Kim et al. [18] studied the effect of air stoichiometry on dynamic performance of PEMFC under load change. The results of their experiments indicated that when loading off and loading on, overshoot and undershoot behavior will occur, respectively.

To study the effects of dynamic loading on fuel cell stacks, the measuring methods of current distribution and temperature distribution are developed in this paper. The current distribution, temperature distribution, and their dynamic changes inside fuel cell stack during dynamic loading have been observed in situ.

### 2. Experimental

#### 2.1. Preparation of mini-size thermocouples

The mini-size thermocouples were prepared using a pair of 0.1 mm copper–constantan thermocouple wires. One end was

\* Corresponding author. Tel.: +86 411 8437 9587; fax: +86 411 8437 9185.  
E-mail addresses: [xqyan@dicp.ac.cn](mailto:xqyan@dicp.ac.cn) (X. Yan), [houting@dicp.ac.cn](mailto:houting@dicp.ac.cn) (M. Hou).

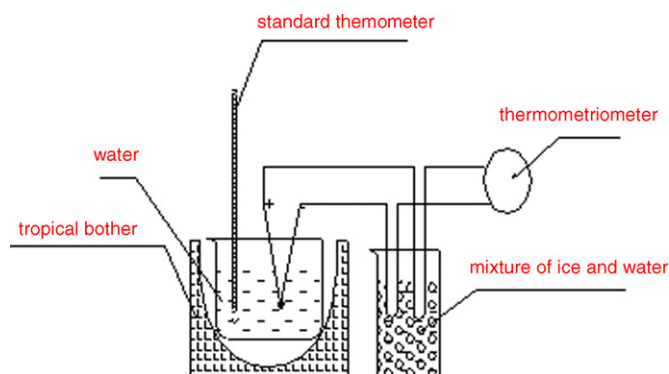


Fig. 1. The schematic drawing of mini-size thermocouples calibration.

welded as the working end (hot end) for measuring inside fuel cell temperature and another end (cool end) was taken as reference end. The mini-size thermocouples were calibrated before being used. The method of calibration is shown in Fig. 1. The cool end was embedded in a mixture of ice and water keeping  $0^{\circ}\text{C}$  and the hot end and a standard thermometer were put into a simulating working medium. The prepared mini-size thermocouples were demarcated under different temperatures. The results are shown in Fig. 2.

## 2.2. Installation of thermocouples in the stack and measurements of temperature distribution

A 16-cell stack was assembled using metal composite bipolar plates and MEAs. The metal composite bipolar plates included thin metal plates served as the separators and the flow fields that were parallel channel pattern formed by stamped method using expanded graphite plates. While, the MEAs consisted of Nafion 212 membranes, catalyst layers with a total Pt loading of  $0.8\text{ mg cm}^{-2}$ , and Toray paper as gas diffusion layers. The active area of MEA was  $270\text{ cm}^2$ . Three mini-size thermocouples were embedded in the upper surfaces of the cathode flow field at the eighth cell of stack in Fig. 3.

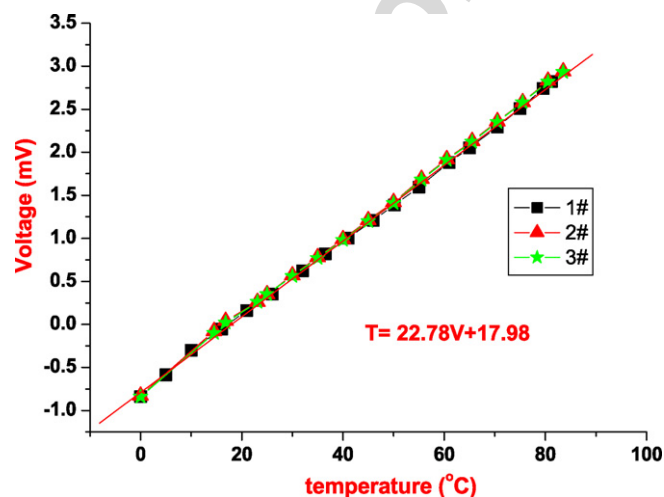


Fig. 2. The calibrating results of mini-size thermocouples.

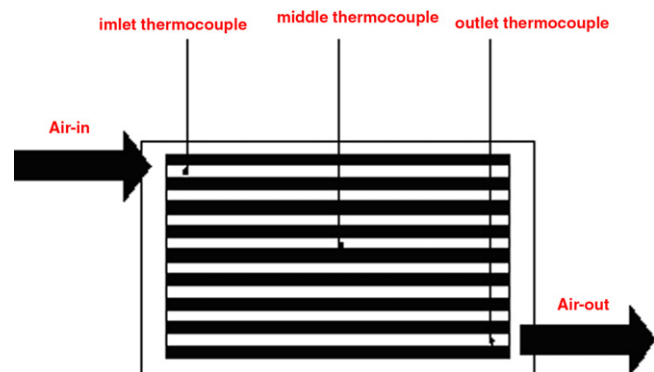


Fig. 3. Schematic diagram of positions of mini-size thermocouple on the cathode flow field plate.

The experiments were conducted in the auto mode, using a 36 kW Fuel Cell Test Station (FCATS-H36000, Hydrogenics, Canada) and a water-cooled electronic load system from TDI (WCL488400-1000-12000) that had a maximum current of 1000 A. The loading response time of this electronic load was short, less than 0.1 s from 0 to  $500\text{ mA cm}^{-2}$ . The hydrogen and air flow rates were controlled by smart mass flow. The hydrogen and air were humidified using high-pressure steam. The relative humidity of anode and cathode sides was accurately adjusted by changing dew point temperature. The operation temperature and pressure of stack was kept at  $60^{\circ}\text{C}$  and ambient pressure.

## 2.3. Measurement of current distribution

The measurement of current distribution inside a single fuel cell is set up. To measure current distribution, the cathode flow field was segmented. The 15 graphite segments ( $23.2\text{ mm} \times 62\text{ mm}$ ) were integrated into the endplate made of organic glass in Fig. 4. Each segment was connected with a separate current output line. Current was measured using a current mutual inductance element. The MEA and anode flow field are the same with those used in measuring temperature distribution. The current distribution of fuel cell was measured using the electronic load (PLZ664WA, Kikusui Electronics, Japan).

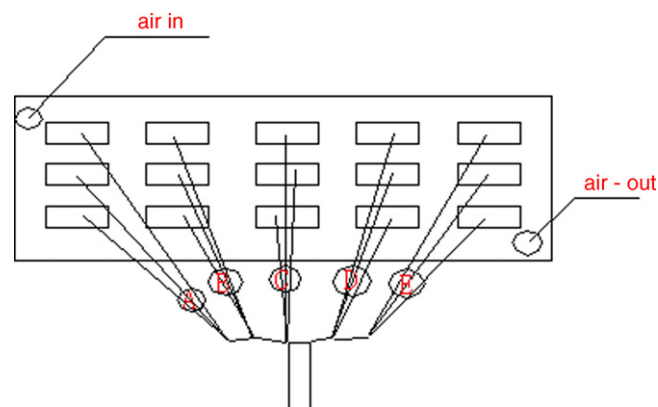


Fig. 4. Schematic diagram of current distribution measurement.

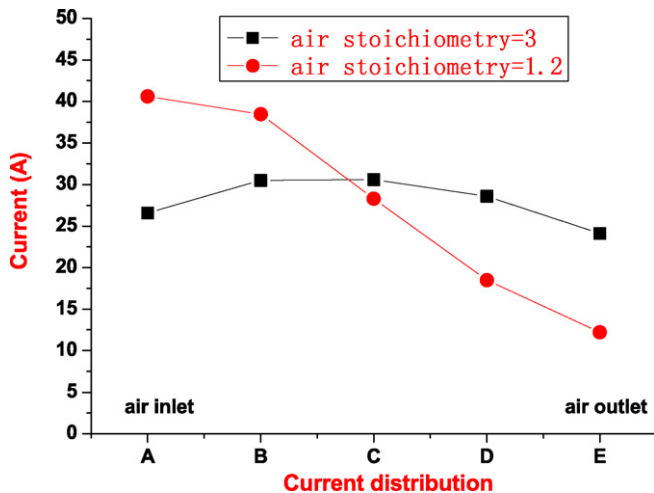


Fig. 5. Current distribution of different positions inside the fuel cell at loading  $500 \text{ mA cm}^{-2}$ .

### 3. Results and discussion

#### 3.1. Current distribution under different air stoichiometries

Fig. 5 gives the current distribution of different positions inside the fuel cell at a fixed loading. It can be seen that the currents are different at different positions along the air flow direction. Also at different air stoichiometries, the current distributions are different. At the low air stoichiometry of 1.2, the current near the cathode inlet is larger than those of other zones. The main cause is that when air stoichiometry is very low, the oxidant starvation occurs near the cathode outlet which leads to the reaction resistance increases near the cathode outlet. So the current reduces dramatically near the cathode outlet. As constant current mode has been adopted, the current near the cathode inlet increases dramatically.

On the other hand, at the high air stoichiometry of 3, the oxidant is sufficient for fuel cell, thus near the cathode outlet, the oxidant starvation is not likely to occur. As a result, the current distribution in fuel cell is more uniform.

#### 3.2. The temperature fluctuation in fuel cell with different air stoichiometries during dynamic loading

Fig. 6 describes the temperature fluctuations in different zones during dynamic loading from 0 to  $500 \text{ mA cm}^{-2}$ , air stoichiometry = 1.2. It can be seen that the temperature fluctuations in different zones of fuel cell are different during dynamic loading. As is illustrated in Fig. 5, when the air stoichiometry is very low, the current near the cathode inlet increases dramatically, which results in the dramatic increase of the temperature near the cathode inlet too. While in the moment of dynamic loading, due to the gas response rate lagging the loading rate, the oxidant starvation becomes more severe, in this case, the air stoichiometry is less than 1. The temperature of cathode inlet increases to  $72^\circ\text{C}$ , while the corresponding temperature of cathode outlet is only  $52^\circ\text{C}$ .

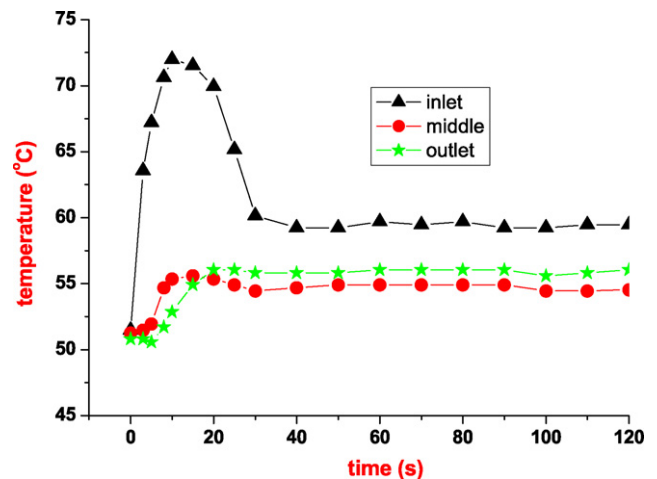


Fig. 6. The temperature fluctuations in different zones during dynamic loading from 0 to  $500 \text{ mA cm}^{-2}$ , air stoichiometry = 1.2.

To better observe temperature fluctuation inside the fuel cell, the temperature change in cathode inlet zone is observed especially. The temperature fluctuations of cathode inlet at different air stoichiometries are shown in Fig. 7. With air stoichiometry decreasing, the oxidant starvation becomes more severe during transient loading, and the highest temperature reached is higher. Also, as shown in Fig. 7, even when the operation reaches steady state, the temperature at low stoichiometry keeps a rather high value too. So increasing air stoichiometry can reduce the extent of temperature change inside fuel cell under dynamic running.

#### 3.3. The temperature fluctuation in fuel cell with different loading rate

Fig. 8 illustrates the transient temperature changes in different zones inside the fuel cell are different with different loading rates. The load change is from 0 to 135 A ( $500 \text{ mA cm}^{-2}$ ). The loading times from 0 to  $500 \text{ mA cm}^{-2}$  are arranged, respectively, for <math>0.1 \text{ s}</math> (response time of electronic load), 1, 3, 5, and 10 s. As

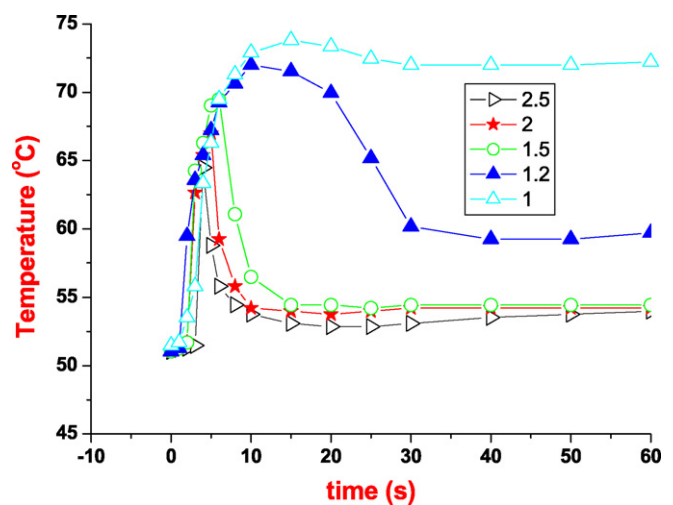


Fig. 7. The temperature fluctuations at cathode inlet with different air stoichiometries, dynamic loading from 0 to  $500 \text{ mA cm}^{-2}$ .

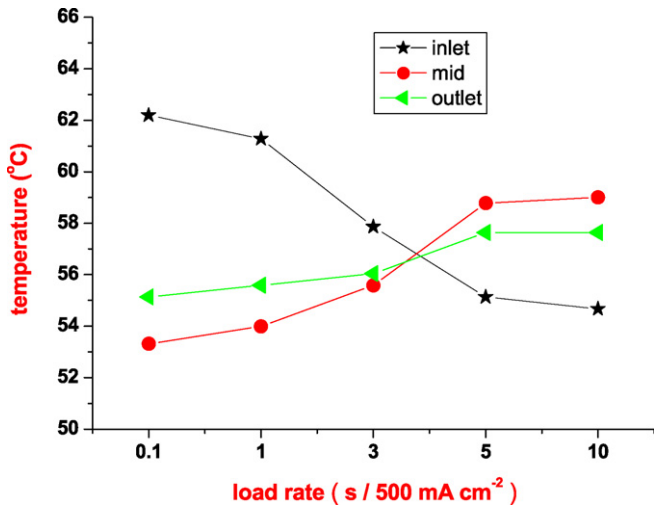


Fig. 8. Transient temperature changes inside the fuel cell with different loading rates, air stoichiometry = 2.0, dynamic loading from 0 to 500 mA cm<sup>-2</sup>.

is shown, with the loading rate decreasing, the transient temperature of cathode inlet reduces, however, the transient temperature of cathode outlet increases. When the loading rate is very fast at 0.1 s/500 mA cm<sup>-2</sup>, the temperature of cathode inlet is much higher than that of cathode outlet. The possible reason is that the loading rate is too fast to result in the oxidant starvation. While the loading rate is slower than 5 s/500 mA cm<sup>-2</sup>, the cathode outlet temperature turns out to be higher than that of cathode inlet. These phenomena can be explained by which air-supplied rate is able to meet the demand of essential air stoichiometry, consequently the oxidant starvation does not occur.

To better understand fuel cell dynamic behavior, the influence of loading rate on the temperature in the cathode inlet is investigated especially. The temperature fluctuations at the cathode inlet with different loading rates are shown in Fig. 9. The faster the loading rate is, the higher the transient temperature is. The air supplying cannot meet the demand of essential stoichiometry when rapid loading. As seen in Fig. 10, the voltage

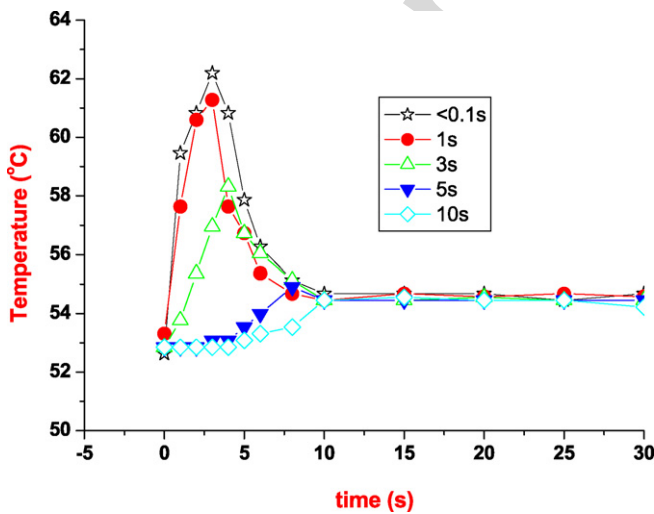


Fig. 9. The temperature fluctuations at cathode inlet with different loading rates, air stoichiometry = 2.0, dynamic loading from 0 to 500 mA cm<sup>-2</sup>.

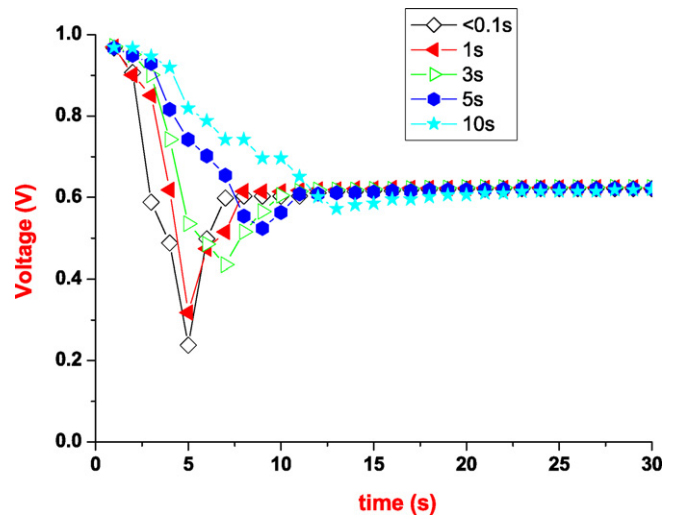


Fig. 10. The performance changes with different loading rates, air stoichiometry = 2.0, dynamic loading from 0 to 500 mA cm<sup>-2</sup>.

of fuel cell stack appears undershoot during transient period of dynamic loading. While the loading rate is quicker, the degree of undershoot is bigger. The cathode potential drops due to the lack of oxygen, and the cell voltage generally drops to very low levels or may even become negative [19]. The experimental results show that the dynamic rapid loading will affect the stability of fuel cell stacks. As a result, in order to improve the stability and lifetime of fuel cell stacks, the dynamic loading rate should be slowed as much as possible.

### 3.4. The temperature change in fuel cell at different loading degrees

Fig. 11 describes the temperature changes at cathode inlet at different loading degrees. As can be seen, the transient temperatures reached are different when the rapid dynamic loading degrees are different. The transient temperature rises obviously when loading degrees enhance. The main reason for this is that

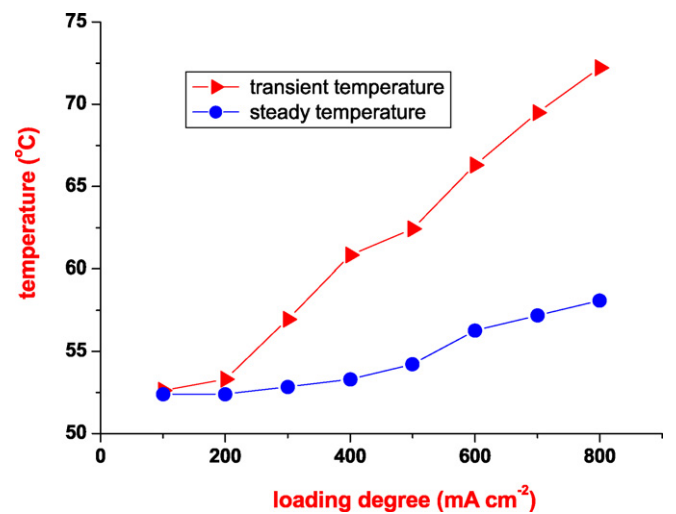


Fig. 11. Temperature changes at cathode inlet at different loading degrees, air stoichiometry = 2.0, loading response time < 0.1 s.

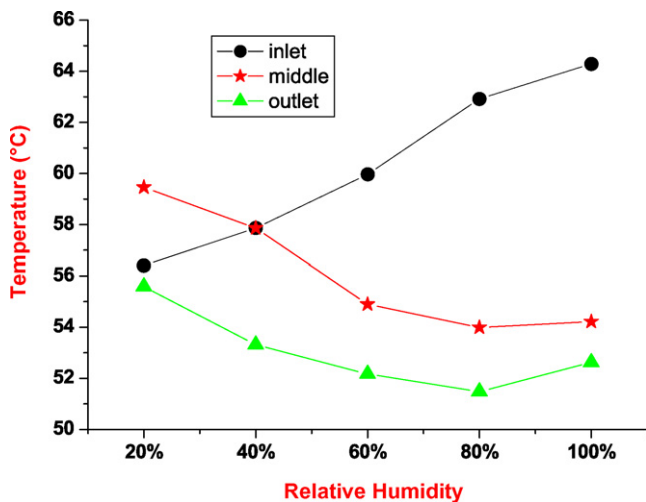


Fig. 12. Transient temperature changes in cathode with different relative humidity levels, dynamic loading from 0 to  $500 \text{ mA cm}^{-2}$ , loading response time < 0.1 s, air stoichiometry = 2.0.

the higher loading degrees result in the more severe oxidant starvation. So the degrees of transient temperature fluctuation enlarge gradually when loading degrees increase.

### 3.5. Transient temperature change in fuel cell with different relative humidity levels during dynamic loading

As seen in Fig. 12, the experimental results show that the transient highest temperature at cathode inlet appears rising when air relative humidity rises during dynamic loading. It is well known that reactant humidity plays a critical role in the performance of PEM fuel cells. When reactant relative humidity is very low, the membrane close to the inlet is relatively dry, in this case the membrane resistance is very high, which leads to a lower current, therefore, the temperature is relatively low. Along the channel direction, more and more water is produced and the membrane becomes better and better hydrated, thus the current increases, so does the temperature. Hereby the temperature in the middle of cathode is larger than the temperature of cathode inlet. While in the cathode outlet, as the oxidant concentration is lower or the oxidant starvation occurs, the current decreases, so the temperature of cathode outlet is low. When reactant relative humidity is increasing, the membrane at inlet becomes better hydrated and its resistance decreases, thus the current increases gradually, so does the temperature, however, as constant current mode is adopted, the currents both in the middle and outlet area of cathode decrease gradually, and the corresponding temperatures decrease gradually too.

## 4. Conclusions

The measuring methods of current distribution and temperature distribution are developed. In this paper, the current

distribution and temperature distribution as well as their dynamic changes have been observed in situ. The experimental results show that the local current and temperature near the cathode inlet rise evidently when dynamic loading, air stoichiometries, loading rates, loading degrees, and air relative humidities have significant effects on the temperature inside the fuel cell during dynamic loading. At low air stoichiometry, the temperatures of cathode inlet rise sharply during dynamic loading. During the transient period of dynamic loading, the quicker the loading rate is, the bigger the extent of temperature fluctuation is. The temperature changes during dynamic loading are different at different air relative humidities. With the increasing of air relative humidity, the transient temperature of cathode inlet rises, while the transient temperature of cathode outlet decreases. The main reason to the above experimental phenomena is that the oxidant starvation occurs during rapid dynamic loading due to the gas response rate lagging the loading rate. Both increasing air stoichiometry and reducing loading rates can improve the uniformity of current and temperature distribution in fuel cell stack during rapid dynamic loading. The experimental results can provide reference for durability researches on FCVs.

## References

- [1] S. Srinivasan, D.J. Manko, H. Koch, M.A. Enayetullah, J.A. Appleby, J. Power Sources 29 (1990) 367–387.
- [2] V. Mehta, J.S. Cooper, J. Power Sources 114 (2003) 32–53.
- [3] A.F. Ghenciu, Solid State Mater. 6 (2002) 389–399.
- [4] P. Costamagna, S. Srinivasan, J. Power Sources 102 (2001) 242–252.
- [5] R.A. Lemons, J. Power Sources 29 (1990) 251–264.
- [6] C. Pan, R. He, et al., J. Power Sources 145 (2005) 392–398.
- [7] J. Hana, S.M. Leea, H. Chang, J. Power Sources 112 (2002) 484–490.
- [8] B.C.H. Steele, J. Mater. Sci. 36 (2001) 1053–1068.
- [9] J. T. Pukrushpan, A.G. Stefanopoulou, H. Peng, Springer, ISBN: 1-85233-816-4 (XVII), 2004.
- [10] S. Kim, S. Shimpalee, J.W. Van Zee, J. Power Sources 137 (2004) 43–52.
- [11] S. Kim, S. Shimpalee, J.W. Van Zee, J. Power Sources 135 (2004) 110–121.
- [12] S. Pischinger, C. Schönfelder, J. Ogrzewalla, J. Power Sources 135 (2004) 110–121.
- [13] J. Hamelin, K. Agbossou, A. Laperriere, F. Laurencelle, T.K. Bose, Int. J. Hydrogen Energy 26 (2001) 625–629.
- [14] J.C. Amphlett, E.H. De Oliveria, R.F. Mann, P.R. Roberge, A. Rodrigues, J.P. Salvador, J. Power Sources 65 (1997) 173–178.
- [15] J.C. Amphlett, R.F. Mann, B.A. Peppley, P.R. Roberge, A. Rodrigues, J. Power Sources 61 (1997) 183–188.
- [16] B. Emonts, J. Bøgild Hansen, H. Schmidt, T. Grube, B. Hohlein, R. Peters, A. Tschauder, J. Power Sources 86 (2000) 228–236.
- [17] F. Philipps, G. Simons, K. Schiefer, J. Power Sources 154 (2006) 412–419.
- [18] S. Kim, S. Shimpalee, J.W. Van Zee, J. Power Sources 135 (2004) 110–121.
- [19] S.D. Knights, K.M. Colbow, J. St-Pierre, D.P. Wilkinson, J. Power Sources 127 (2004) 127–133.